Multiuser Precoding for UWB Sensor Networks

Heinrich Luecken and Armin Wittneben
Communication Technology Laboratory, ETH Zurich, 8092 Zurich, Switzerland
{lueckenh, wittneben}@nari.ee.ethz.ch

***Abstract*—We consider the downlink of an Ultra-Wideband (UWB) sensor network, i.e. communication from a central unit to many sensor nodes. The key to achieve low-complexity, low-power and low-cost sensor nodes are non-coherent receivers. Conventionally, their detection performance strongly suffers from inter-symbol interference due to multipath, which substantially limits the data rate or requires expensive receiver post-processing. To overcome this problem, we propose a novel precoding scheme to transmit to several nodes simultaneously. This way the sum data rate can be increased, while low complexity of sensor nodes is maintained. Specifically, we consider nodes with generalized energy detection receivers and transmission of pulse position modulated data. First, precoding optimization is derived from a Signal-to-Interference-plus-Noise Ratio (SINR) expression for this setup based on full channel state information. To achieve the best sensor network coverage, the minimum SINR of all nodes is maximized. In a second step, optimization is extended to statistical channel knowledge, which depends on the position of the nodes. Performance evaluation based on an extensive measurement campaign shows that multiple nodes can efficiently be served simultaneously. Only marginal increase in transmit power is necessary compared to time-multiplexing.**

I. Introduction

Low cost, small form factor and very low energy consumption – the major challenges of wireless sensor networks (WSN) can be met by Ultra-Wideband (UWB) technology [1]. In particular for short range communication, impulse radio with pulse position modulation (PPM) and energy detection (ED) is well-known for its hardware efficient implementation [2], [3]. Besides robustness to multipath and no demands on channel knowledge, the key advantage of ED-receivers is that their main part can be implemented in an analog fashion, thus avoiding high speed analog-to-digital conversion. In [4], such a receiver has been presented with an estimated average power consumption of less than 1 mW.

The large frequency diversity enables reliable non-coherent UWB communication even in harsh propagation environments, as they are typical for WSN in industrial automation, engines and machinery or in-vehicular communication. However, with increasing data rate, non-coherent detection of UWB signals becomes difficult due to inter-symbol interference (ISI) from multipath. For very low-complexity energy detection receivers, the symbol timing is basically limited by the delay spread of the channel, which leads to a paradox situation: Only low data rates can be achieved, even though several Gigahertz of bandwidth are available. For dense sensor networks with numerous nodes, this may result in severe restrictions on the per node throughput. To increase the throughput while maintaining the low-complexity receiver, we propose a precoding scheme to transmit several data streams simultaneously. The network we consider consists of a central unit that communicates to a large number of sensor nodes (SNs), each equipped with a generalized energy detection receiver.

In this paper, we derive a Signal-to-Interference-plus-Noise Ratio (SINR) expression for the pulse position modulated downlink communication with UWB generalized energy detection receivers. Based on this, we formulate the optimization problem to maximize the minimum SINR of all nodes. This is converted to a quasi-convex problem, which can be solved by standard algorithms. Moreover, we extend the precoding optimization to statistical channel knowledge, i.e. the auto-correlation of the channel impulse response. This enables optimization of simultaneous transmission to nodes located in different regions and saves channel estimation overhead. The performance of the proposed precoding scheme is evaluated based on measurements.

In literature, ISI suppression with transmitter as well as receiver processing has extensively been studied for single user UWB systems. At the receiver side, non-coherent detectors that account for ISI [5] or MLSE post-detection [6] have been derived. However, this is too complex for the use in SNs. Prominent approaches for transmitter optimization are time reversal [7], channel phase precoding [8], [9], and pre-equalization [10], which also takes the FCC spectral mask constrains into account. However, none of these approaches incorporate the characteristic of a generalized energy detection receiver into optimization. Precoding for these receivers has been introduced in [11] and [12], which is now being extended to multiuser communication.

The remainder of this paper is structured as follows. In Section II, the system model is described. Section III introduces the considered SINR expression, which is optimized in Section IV. The performance evaluation is presented in Section V and conclusions are drawn in Section VI.

II. System Model

The system model we consider in this paper is shown in Fig 1. The transmitter simultaneously sends N streams of pulse position modulated data, i.e. a pulse is transmitted in the first half of the timeslot for a “0” and in the second half for a “1”. Hence, the transmitter inputs $b_1(t), \ldots, b_N(t)$ are given by

$$b_k(t) = \sum_l c_l \delta\left(t - a_k[l]T_{\text{ppm}} - lT_{\text{symb}}\right), k = 1, \ldots, N.$$

The transmit data of time-slot l, which is intended for node k is denoted by $a_k[l]$. We assume equiprobable $a_k[l] \in \{0, 1\}$,

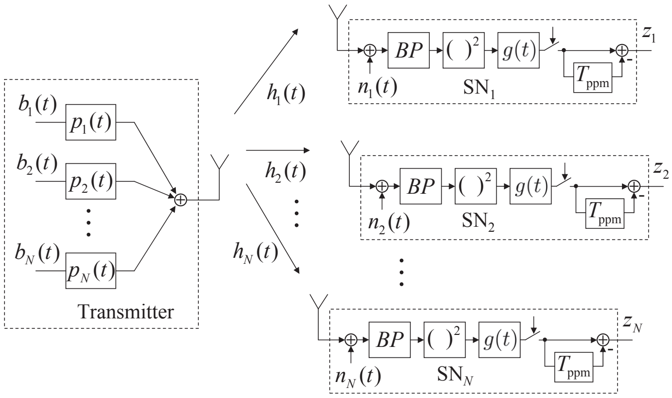

Fig. 1. System model

which are i.i.d. for all $k = 1, \dots, N$ and time-slots l. The symbol duration is given by T_{symb} and the pulse shift by $T_{\text{ppm}} = T_{\text{symb}}/2$. Note that the polarity of the pulses is scrambled by random $c_l \in \{-1, 1\}$ to avoid discrete lines in the transmit spectrum. The data streams are linearly precoded by a convolution with $p_1(t), \dots, p_N(t)$, respectively, and then they are added up and transmitted over the same transmit antenna. The multipath channel to node k is characterized by its impulse response $h_k(t)$. At each receiver, the signal is perturbed by independent white Gaussian noise with power spectral density $N_0/2$. The generalized energy detection receiver consists of a bandpass, a squaring device and a post-detection filter with impulse response $g(t)$, which performs the integration. Two samples per symbol are taken at the output and subtracted, which leads to the decision variable z_k. If z_k is greater than zero, node k decides for a "0" and if it is less than zero, it decides for a "1". In the following, we consider only one time-slot and omit the index l.

III. Signal-to-Interference-plus-Noise Ratio

For the derivation[1] of an SINR expression of this setup, the continuous time signals are sampled with sufficiently high sampling frequency $f_s = 1/T_s$ and we assume that edge effects are negligible. In vector notation, the receiver output for node k can be written as:

$$z_k = \mathbf{g}^T \left[\left(\sum_{i=1}^{N} a_i \mathbf{H}_k \mathbf{p}_i + \mathbf{n}_k \right) \odot \left(\sum_{j=1}^{N} a_j \mathbf{H}_k \mathbf{p}_j + \mathbf{n}_k \right) \right] - \mathbf{g}^T \left[\left(\sum_{i=1}^{N} \bar{a}_i \mathbf{H}_k \mathbf{p}_i + \mathbf{n}'_k \right) \odot \left(\sum_{j=1}^{N} \bar{a}_j \mathbf{H}_k \mathbf{p}_j + \mathbf{n}'_k \right) \right] \quad (1)$$

[1]*Notation:* Boldface lowercase and uppercase letters indicate column vectors and matrices, respectively. $(\cdot)^T$, $\odot$, $\otimes$, $\mathsf{E}[\cdot]$, $\|\cdot\|_1$ denote transposition, Hadamard and Kronecker product, expectation, and ℓ_1-norm, respectively. The N-by-N identity matrix and N-by-N-matrix of zeros are written as $\mathbf{I}_N$ and $\mathbf{0}_N$. The largest generalized eigenvalue of the matrices $\mathbf{A}$ and $\mathbf{B}$ is denoted by $\lambda_{\max}\{\mathbf{A}, \mathbf{B}\}$ and the corresponding generalized eigenvector by $\mathbf{v}_{\max}\{\mathbf{A}, \mathbf{B}\}$.

The first line corresponds to the pulses that are transmitted in the first half of the time-slot and the second line to the second half, where $\bar{a}_i := 1 - a_i$, $i = 1, \dots, N$. All vectors are of dimension $(M \times 1)$ with $M = T_{\text{ppm}}/T_s$: the transmit pulses $\mathbf{p}_i = [p_i(T_s), \dots, p_i(MT_s)]^T$, the noise of the first and the second half of the time-slot $\mathbf{n}_k, \mathbf{n}'_k \sim \mathcal{N}(\mathbf{0}, \mathbf{\Sigma}_{nn})$ and the post-detection filter $\mathbf{g} = [g(MT_s), \dots, g(T_s)]^T$, which is stacked into the vector in reverse order. The $(M \times M)$-channel matrix $\mathbf{H}_k$ has Toeplitz structure with the zero-padded and shifted channel impulse response $[h_k(T_s), \dots, h_k(MT_s)]^T$ on its columns. The bandpass is incorporated into the channel impulse response and the covariance matrix of the noise $\mathbf{\Sigma}_{nn}$. Note that this input-output relation does not account for ISI of the single data streams. It is assumed that the channel excess delay is smaller than half of the symbol time-slot. This is a reasonable assumption for the derivation of the precoding optimization, because we aim to increase the sum data rate by simultaneous transmission to several nodes. This keeps the per node data rate small.

Expanding the element-wise multiplication and rearranging terms of (1) yields

$$\begin{aligned} z_k = &\sum_{i=1}^{N} \sum_{j=1}^{N} (a_i a_j - \bar{a}_i \bar{a}_j) \mathbf{p}_i^T \mathbf{H}_k^T \mathbf{G} \mathbf{H}_k \mathbf{p}_j \\ &+ 2\mathbf{g}^T \left(\sum_{i=1}^{N} (a_i \mathbf{n}_k - \bar{a}_i \mathbf{n}'_k) \odot \mathbf{H}_k \mathbf{p}_i \right) \\ &+ \mathbf{g}^T \left(\mathbf{n}_k \odot \mathbf{n}_k - \mathbf{n}'_k \odot \mathbf{n}'_k \right), \end{aligned} \quad (2)$$

where $\mathbf{G} = \operatorname{diag}(\mathbf{g})$. The first line corresponds to the squared signal terms, the second line to the mixed signal and noise terms, and the third line to the squared noise. To keep the problem tractable, we neglect the mixed term for the precoding optimization, which corresponds to a low SNR approximation. The SINR-expression γ_k for node k that we use for optimization is defined as

$$\gamma_k = \frac{\mathbf{p}_k^T \mathbf{H}_k^T \mathbf{G} \mathbf{H}_k \mathbf{p}_k}{\sum_{i \neq k} \sum_{j \neq k} \sigma_{ij} \mathbf{p}_i^T \mathbf{H}_k^T \mathbf{G} \mathbf{H}_k \mathbf{p}_j + \sigma_n^2}, \quad (3)$$

where $\sigma_{ij} = 1$ for $i = j$, and $\sigma_{ij} = 1/2$ for $i \neq j$. The numerator contains the desired signal component, whereas the denominator collects the interference terms and the noise term σ_n^2, which is independent of $\mathbf{p}_i$ and proportional to N_0.

IV. Precoding Optimization

The objective for optimization can be various, depending on application, quality of service requirements, channel characteristics, or number of nodes. Common approaches include to maximize either the sum-performance of the network or the performance of a subset of the considered nodes. In this paper, we consider the fundamental case to guarantee the best performance for the weakest node. This increases the coverage of the sensor network, since nodes with bad channel conditions can gain from nodes with good channel conditions. In other words, the optimization problem we aim to solve can be formulated as follows:

$$\max_{\mathbf{p}_1,\ldots,\mathbf{p}_N} \min_{k=1,\ldots,N} \gamma_k \ , \qquad \text{s.t.} \qquad E_p = 1 \tag{4}$$

The given constraint limits the average total transmit energy per time-slot E_p, which is given by

$$E_p = \frac{1}{f_s} \sum_{i=1}^{N} \sum_{j=1}^{N} \mathsf{E}\left[a_i a_j + \bar{a}_i \bar{a}_j\right] \mathbf{p}_i^T \mathbf{p}_j.$$

Stacking all transmit pulses into one large vector $\bar{\mathbf{p}}$, the normalized transmit power can be written as

$$E_p = \bar{\mathbf{p}}^T (\mathbf{C} \otimes \mathbf{I}_M) \bar{\mathbf{p}}, \text{ with } \bar{\mathbf{p}} = \left[\mathbf{p}_1^T, \ldots, \mathbf{p}_N^T\right]^T.$$

The $(i,j)^{\text{th}}$-component of the $(N \times N)$-matrix $\mathbf{C}$ is given by

$$[\mathbf{C}]_{i,j} = \frac{1}{f_s} \mathsf{E}\left[a_i a_j + \bar{a}_i \bar{a}_j\right] = \begin{cases} T_s & \text{for } i = j \\ T_s/2 & \text{for } i \neq j. \end{cases}$$

The objective function γ_k for node k can be written as a generalized Rayleigh quotient by inclusion of the power constraint. With the substitution

$$\bar{\mathbf{p}} \mapsto \frac{\tilde{\mathbf{p}}}{\sqrt{\tilde{\mathbf{p}}^T (\mathbf{C} \otimes \mathbf{I}_M) \tilde{\mathbf{p}}}},$$

the power constraint is fulfilled for all $\tilde{\mathbf{p}} \in \mathbb{R}^{NM}$. Hence, the optimized precoding vector $\tilde{\mathbf{p}}^*$ can be formulated as

$$\tilde{\mathbf{p}}^* = \arg\max_{\tilde{\mathbf{p}} \in \mathbb{R}^{NM}} \min_{k=1,\ldots,N} \frac{\tilde{\mathbf{p}}^T \mathbf{A}_k \tilde{\mathbf{p}}}{\tilde{\mathbf{p}}^T \mathbf{B}_k \tilde{\mathbf{p}}}. \tag{5}$$

The $(NM \times NM)$-matrix $\mathbf{A}_k$ and $\mathbf{B}_k$ in the numerator and in the denominator, respectively, are given by

$$\begin{aligned} \mathbf{A}_k &= \mathbf{E}_k \otimes (\mathbf{H}_k^T \mathbf{G} \mathbf{H}_k) \\ \mathbf{B}_k &= \mathbf{F}_k \otimes (\mathbf{H}_k^T \mathbf{G} \mathbf{H}_k) + \sigma_n^2 \mathbf{C} \otimes \mathbf{I}_M. \end{aligned}$$

The $(N \times N)$-matrix $\mathbf{E}_k$ is all zero except for $[\mathbf{E}_k]_{k,k} = 1$ and the $(N \times N)$-matrix $\mathbf{F}_k$ is 1 on its main diagonal and $1/2$ elsewhere, with the k^{th}-column and k^{th}-row being zero:

$$[\mathbf{F}_k]_{i,j} = \begin{cases} 1 & \text{for} \quad i = j \text{ and } j \neq k \\ 1/2 & \text{for} \quad i \neq j \text{ and } i \neq k \text{ and } j \neq k \\ 0 & \text{for} \quad i = k \text{ or } j = k. \end{cases}$$

As shown in [13], the problem (5) can be converted to the search of the minimal principal generalized eigenvalue of the convex combination of the matrices $\mathbf{A}_k$ and $\mathbf{B}_k$:

$$\boldsymbol{\mu}^* = \arg\min_{\boldsymbol{\mu} \in [0,1]^N : \|\boldsymbol{\mu}\|_1 = 1} \lambda_{\max} \left\{ \sum_{k=1}^{N} \mu_k \mathbf{A}_k, \sum_{k=1}^{N} \mu_k \mathbf{B}_k \right\}, \tag{6}$$

where $\boldsymbol{\mu} = \left[\mu_1, \ldots, \mu_N\right]^T$. Note that this problem is quasi-convex and the search over $\boldsymbol{\mu}$ is only of dimension $N-1$, e.g. for two nodes the optimization problem results in a line search. Eventually, the optimal transmit pulses are then given by

$$\tilde{\mathbf{p}}^* = \mathbf{v}_{\max} \left\{ \sum_{k=1}^{N} \mu_k^* \mathbf{A}_k, \sum_{k=1}^{N} \mu_k^* \mathbf{B}_k \right\}. \tag{7}$$

Statistical Channel Knowledge: To extend the precoding to statistical channel knowledge, the channel impulse response is modeled as a non-stationary random process, i.e. $[h_k(T_s), \ldots, h_k(MT_s)]^T$ is a random vector with covariance matrix $\boldsymbol{\Sigma}_h$ and mean $\boldsymbol{\mu}_h$. In particular, this is useful for two different scenarios: i) to model noisy or outdated channel state information and ii) to perform location-aware precoding. If the coverage area of the network is divided into small regions, a characteristic parameter set of $\boldsymbol{\Sigma}_h$ and $\boldsymbol{\mu}_h$ can be estimated for each region. Thus, the precoding can be optimized depending on the position of the node, i.e. for its region exhibiting a certain multipath propagation characteristic.

To obtain an SINR expression based on statistical channel knowledge, the expectation of the receiver output (2) is taken with respect to the channel. This corresponds to taking the expectation of the numerator and the denominator of the objective function of (5) with respect to $\mathbf{H}$. In doing so, the structure of the optimization problem is not changed, only the values of matrices in the numerator and denominator are different. They are given by

$$\begin{aligned} \hat{\mathbf{A}}_k &= \mathbf{E}_k \otimes \mathsf{E}[\mathbf{H}_k^T \mathbf{G} \mathbf{H}_k] \\ \hat{\mathbf{B}}_k &= \mathbf{F}_k \otimes \mathsf{E}[\mathbf{H}_k^T \mathbf{G} \mathbf{H}_k] + \sigma_n^2 \mathbf{C} \otimes \mathbf{I}_M. \end{aligned}$$

The (i,j)th-element of $\mathsf{E}[\mathbf{H}_k^T \mathbf{G} \mathbf{H}_k]$ is given by

$$\left[\mathsf{E}[\mathbf{H}_k^T \mathbf{G} \mathbf{H}_k]\right]_{i,j} = \sum_{l=1}^{M} \mathsf{E}\left[[\mathbf{H}_k]_{l,i} [\mathbf{H}_k]_{l,j}\right] [\mathbf{G}]_{l,l}.$$

These values depend only on the covariance matrix $\boldsymbol{\Sigma}_h$ and mean $\boldsymbol{\mu}_h$ of the channel impulse response and on the post-detection filter. The optimized transmit pulses based on statistical channel knowledge are then given by (6) and (7) with $\mathbf{A}_k \mapsto \hat{\mathbf{A}}_k$ and $\mathbf{B}_k \mapsto \hat{\mathbf{B}}_k$.

V. Performance Evaluation

To evaluate the performance of the proposed precoding scheme, we simulate the system as it is described in Section II and use precoding as introduced in Section IV. As figure of merit, we consider the average bit-error-rate (BER).

The performance evaluation is based on an extensive measurement campaign. The channel impulse responses have been measured in an indoor environment with dense multipath in line-of-sight (LOS) as well as non-line-of-sight (NLOS) situations. A floorplan of the measurement environment is plotted in Fig. 3. The transmitting central unit is denoted by CH (cluster head) and the measurement area is divided into 22 regions of size 27 cm × 56 cm each. Per region $N_h = 620$ channel impulse responses are measured by moving the receiving antenna on an equidistant horizontal grid. All antenna and hardware effects are assumed to be included in the channel impulse response. The measurement setup is described in detail in [14]. All channel impulse responses are aligned to the maximum of their absolute envelope.

The system we consider for performance evaluation has a transmission bandwidth of $B = 3\,\text{GHz}$ at center frequency of $f_c = 4.5\,\text{GHz}$. The symbol timing is $T_{\text{symb}} = 100\,\text{ns}$,

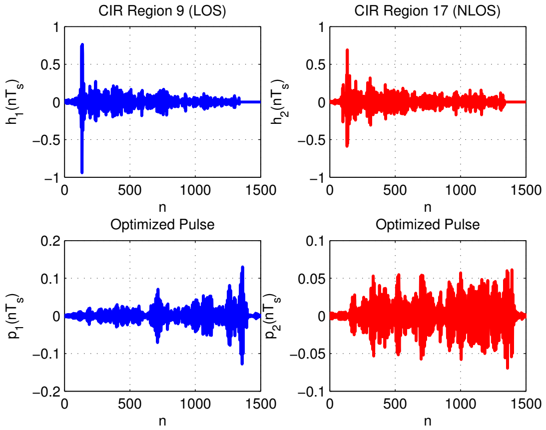

Fig. 2. Channel impulse response vectors from region 9 (LOS) and 17 (NLOS) and resulting precoding vectors for two nodes.

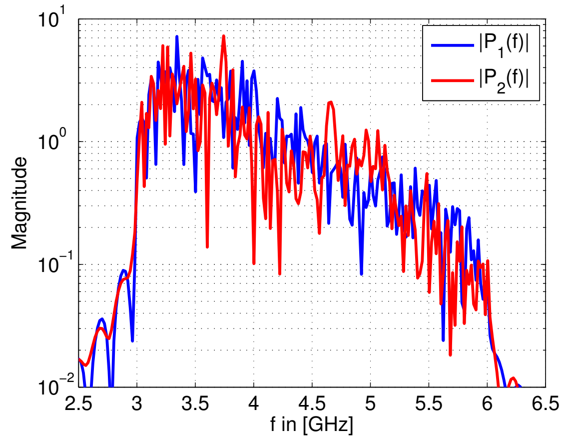

Fig. 4. Normalized spectrum of optimized precoding pulses $p_1(t)$ and $p_2(t)$ for region 9 and 17, respectively.

which results in a per node data rate of 10 Mbps. To account for stringent complexity requirements of the SNs, the post-detection filter is chosen as first-order low-pass filter with impulse response $g(t)$ given by

$$g(t) = \begin{cases} g_0 \exp\left(-t2\pi f_{\text{cutoff}}\right) & \text{for } t > 0 \\ 0 & \text{else,} \end{cases}$$

with scaling coefficient g_0 and the cutoff frequency set to $f_{\text{cutoff}} = 50\,\text{MHz}$. The band-pass filter at the receiver input is assumed to be perfectly band limiting for the considered transmission band from 3 to 6 GHz. The simulation sampling frequency is chosen to $f_s = 30\,\text{GHz}$, which results in precoding vectors of dimension $M = 1500$.

Fig. 2 (top) shows a channel impulse response from a LOS position and one from a NLOS position. Note that we normalize the channel impulse responses to unit energy to suppress the influence of pathloss. Below, the two-user precoding vectors are plotted for two nodes with the corresponding channels. Fig. 4 shows the normalized magnitude spectrum of this precoding pulses. The optimization results are for $E_p/N_0 = 12\,\text{dB}$, where E_p denotes the average total transmit energy per time-slot and N_0 the spectral noise density.

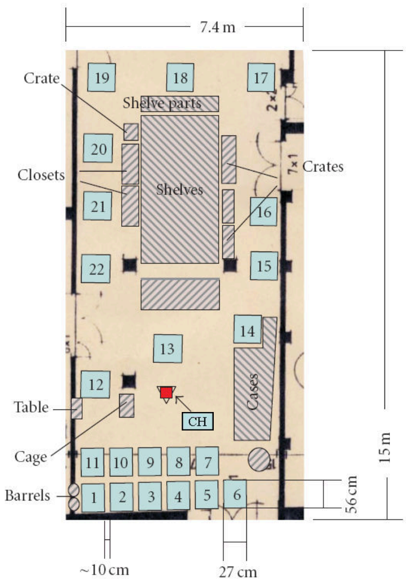

Fig. 3. Floor plan of measurement area

First, the performance of multiuser precoding with full channel knowledge is evaluated. We assume static channels for a blocksize of 256 bits, which are randomly drawn from region 9, 17, 20, and 11 with one user in each region. The BER is averaged across channel realizations and users. In Fig. 5, the average BER is plotted with precoding optimization for single user and $N = 2, 3$ and 4 (no marker, triangle, square, and circle, respectively). The dashed line plots the average BER without precoding, i.e. a single ideal bandpass pulse of energy E_p is used for transmission. The simulations show that the multiuser precoding (blue curves) can effectively orthogonalize the data streams. At high E_p/N_0, the performance penalty from single user to two users is only 3.4 dB, and between two and four users it is still only 4.1 dB. Note that the abscissa carries the total energy per time-slot of all data streams. Hence, time division multiplexing (TDMA, cyan) leads to a performance difference of 3.01 dB since E_p/N_0 needs to be doubled to serve two users instead of one. This shows that compared to time multiplexing, only about 0.4 dB extra transmit power is necessary, whereas the sum data rate is increased by a factor of two. Moreover, with 1.1 dB additional transmit power, the sum data rate can be quadruplicated.

For the single user case, the precoding vector is given by $\mathbf{p}^* = \mathbf{v}_{\max}\left\{\mathbf{A}_1, \mathbf{I}_M\right\}$. For the multiuser optimization, we use in the SINR expression (3) for σ_n^2 the standard deviation of the squared noise term. The simulations show that this leads to the best performance in terms of BER. Thus, we have

$$\sigma_n^2 = 2\left(\mathbf{g}^T(\mathbf{\Sigma}_{nn} \odot \mathbf{\Sigma}_{nn} - \mathbf{\Sigma}_{n'n} \odot \mathbf{\Sigma}_{n'n})\mathbf{g}\right)^{1/2},$$

where $\mathbf{\Sigma}_{nn}$ denotes the covariance of the bandpass-filtered

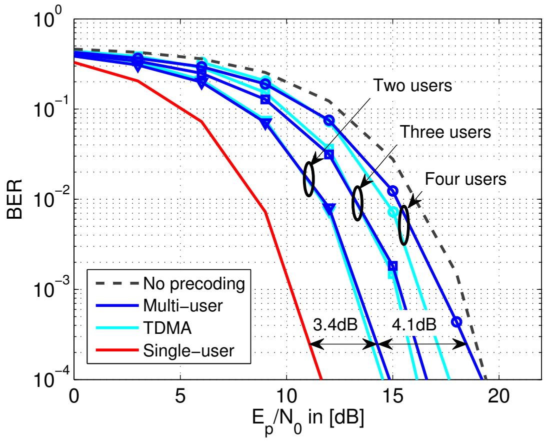

Fig. 5. Average bit error rate for precoding with full channel knowledge (Region 9, 17, 20, and 11).

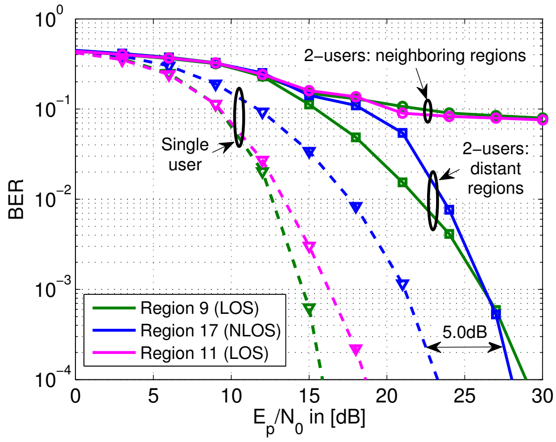

Fig. 6. Average bit error rate for precoding regional channel knowledge.

noise and $\mathbf{\Sigma}_{n'n} = \mathsf{E}[\mathbf{n}_k \mathbf{n}'^T_k]$ the correlation matrix of the noise of the first and the second half of the time-slot, respectively.

Fig. 6 shows the averaged BER performance of the precoding with statistical channel knowledge. For each region, the covariance matrix and mean of the channel impulse responses are estimated with the measurement data. The precoding is performed accordingly for different combination of regions. The single user transmission with optimization based on regional channel knowledge is plotted with dashed lines. It can be observed that the performance for the LOS regions 9 (green) and 11 (magenta) is better than for the NLOS region 17 (blue). One explanation for this is the stronger variation of multipath components in the NLOS case, which makes the precoding more difficult. The solid lines show the performance of precoding optimization with two nodes, which are located in different regions. The curves marked with circles correspond to a scenario of two SNs that are located nearby, whereas for the curves marked with squares a setting is chosen with regions further apart. Significant performance difference can be observed. For neighboring regions, the precoding cannot orthogonalize the two data streams and the BER saturates at about 10%. However, for the distant regions 9 and 17 the precoding works well. The SNs can decode their data stream when the transmit power is increased by about 5 dB compared to single user. This shows that multiuser transmission with statistical channel knowledge is possible, if the propagation environment of the SN's regions differs sufficiently, i.e. the SNs are far enough apart.

VI. Conclusions

In this paper, we show that precoding for simultaneous transmission to multiple very low-complexity sensor nodes is a very promising means to increase the sum data rate. Optimization algorithms based on full as well as statistical channel knowledge are derived from an SINR expression, where the low complexity receiver structure is specifically taken into account. Performance evaluations based on measurements in a strong multipath environment prove the practicality of the presented scheme.

References

[1] J. Zhang, P. Orlik, Z. Sahinoglu, A. Molisch, and P. Kinney, "UWB systems for wireless sensor networks," *Proceedings of the IEEE*, vol. 97, no. 2, pp. 313–331, Feb. 2009.

[2] K. Witrisal, G. Leus, G. Janssen, M. Pausini, F. Troesch, T. Zasowski, and J. Romme, "Noncoherent ultra-wideband systems," *IEEE Signal Processing Magazine*, vol. 26, no. 4, pp. 48 –66, July 2009.

[3] L. Stoica, A. Rabbachin, H. Repo, T. Tiuraniemi, and I. Oppermann, "An ultrawideband system architecture for tag based wireless sensor networks," *IEEE Transactions on Vehicular Technology*, vol. 54, no. 5, pp. 1632 – 1645, Sept. 2005.

[4] F. Troesch, C. Steiner, T. Zasowski, T. Burger, and A. Wittneben, "Hardware aware optimization of an ultra low power UWB communication system," *IEEE International Conference on Ultra-Wideband, ICUWB 2007*, pp. 174–179, September 2007.

[5] T. Zasowski, F. Troesch, and A. Wittneben, "Partial channel state information and intersymbol interference in low complexity UWB PPM detection," *IEEE International Conference on Ultra-Wideband, ICUWB 2006*, pp. 369–374, September 2006.

[6] F. Troesch, T. Zasowski, and A. Wittneben, "Non-linear UWB receivers with MLSE post-detection," in *IEEE Vehicular Technology Conference, VTC Spring 2008*, May 2008.

[7] H. T. Nguyen, I. Kovacs, and P. Eggers, "A time reversal transmission approach for multiuser UWB communications," *IEEE Transactions on Antennas and Propagation*, vol. 54, no. 11, pp. 3216 –3224, Nov. 2006.

[8] Y.-H. Chang, S.-H. Tsai, X. Yu, and C.-C. J. Kuo, "Ultrawideband transceiver design using channel phase precoding," *IEEE Transactions on Signal Processing*, vol. 55, no. 7, pp. 3807 –3822, July 2007.

[9] Y.-H. Chang, S.-H. Tsai, X. Yu, and C.-C. Kuo, "Codeword design for ultra-wideband (UWB) precoding," *IEEE Transactions on Wireless Communications*, vol. 9, no. 1, pp. 198 –207, Jan. 2010.

[10] A.-H. Mohsenian-Rad, J. Mietzner, R. Schober, and V. Wong, "Pre-equalization for pre-rake DS-UWB systems with spectral mask constraints," *IEEE Transactions on Communications*, vol. 59, no. 3, pp. 780 –791, March 2011.

[11] H. Luecken, T. Zasowski, C. Steiner, F. Troesch, and A. Wittneben, "Location-aware adaptation and precoding for low complexity IR-UWB receivers," in *IEEE International Conference on Ultra-Wideband, ICUWB 2008*, vol. 3, Sep. 2008, pp. 31–34.

[12] C. Steiner and A. Wittneben, "Cognitive interference suppression for low complexity UWB transceivers," in *IEEE International Conference on Ultra-Wideband, ICUWB 2008*, Sep. 2008.

[13] J. Wagner, "Distributed forwarding in multiuser multihop wireless networks," Ph.D. dissertation, ETH Zurich, 2011.

[14] C. Steiner, "Location fingerprinting for ultra-wideband systems - the key to efficient and robust localization," Ph.D. dissertation, ETH Zurich, 2010.